NASA TECHNICAL TRANSLATION

NASA TT F-272

NASA TT F-272

THEORY OF SHORT WAVE RADIATION FLUXES IN THE REAL ATMOSPHERE

by K. S. Shifrin, I. N. Minin, O. A. Avaste, and N. P. Pyatovskaya

From *Meteorologicheskogo Soveshchaniya,* Vol. 6, 1963.

NATIONAL AERONAUTICS AND SPACE ADMINISTRATION • WASHINGTON, D. C. • OCTOBER 1965

NASA TT F-272

THEORY OF SHORT WAVE RADIATION FLUXES IN THE REAL ATMOSPHERE

By K. S. Shifrin, I. N. Minin, O. A. Avaste,
and N. P. Pyatovskaya

Translation of "Teoriya spektral'nykh potokov korotkovolnovoy radiatsii v real'noy atmosfere."
Meteorologicheskogo Soveshchaniya, Vol. 6, pp. 30-44, 1963.

NATIONAL AERONAUTICS AND SPACE ADMINISTRATION

For sale by the Clearinghouse for Federal Scientific and Technical Information
Springfield, Virginia 22151 – Price $1.00

THEORY OF SHORT WAVE RADIATION FLUXES IN THE REAL ATMOSPHERE

Earlier work is summarized, and a simple theoretical model is developed to account for the behavior of the radiation fluxes in the short wave portions of the spectrum (infrared and visible) from the viewpoint of optical measurements in the clear real atmosphere. The model is devised so as to utilize most effectively those optical and atmospheric state variables which are easily measured (optical thickness, visible range, water content), providing initial parameters to complete the total conception, from which the remaining parameters can be calculated. The model can be used to calculate the intensities and fluxes with an error satisfactory for many practical applications. In formulating the model, the difficulties inherent in attempts to account simultaneously for scattering and absorption are circumvented by treating the visible and infrared parts of the spectrum separately, assuming a predominant scattering mechanism in the former, an absorption mechanism in the latter. A cursory error analysis is given in connection with the comparison of experimental and analytical results.

INTRODUCTION

The body of problems relating to the study of short wave radiation fluxes and their associated optical phenomena is usually treated from two alternate points of view.

1. In actinometry the primary concern is with the energy relations of these fluxes, which are regarded as components of the radiation balance.

2. In atmospheric optics, the same fluxes are studied in terms of the visual impressions that they make on the observer. In this case, attention is centered chiefly on optical effects. Calculating the luminance of the sky and of the haze between object and observer constitutes the most important problem in this area. These calculations are essential to the vital practical problem of viewing objects (horizontally and obliquely) through optical instruments.

In spite of the fact that an extensive literature has been devoted to both aspects of the problem, the authors have been unable to find an acceptable scheme for calculating the spectral fluxes and intensities at altitudes up to 30 km over a wide spectral range of λ, from 0.29 to 4 μ, under conditions closely approximating those observed in the real atmosphere.

It is convenient to divide the investigated spectral range into two

---

*Numbers in the margin indicated pagination in the original foreign text.

intervals (visible and infrared), using the following logical scheme for scattering and absorption:

SPECTRAL REGION	WAVELENGTH	MULTIPLE SCATTERING	ABSORPTION
Visible	$\lambda \leq 0.7\mu$	Accounted for	Disregarded
Infrared . . .	$0.7 < \lambda < 4\mu$	Disregarded	Accounted for

Of particular interest is the investigation of processes in the troposphere and in the lower levels of the stratosphere in that part of the spectrum where the radiation is detectable by thermoelectric pyranometers with glass windows, in other words, the investigation on "pyranometric" fluxes in the twenty-kilometer subzonal layer.

During the last few years, the Main Geophysical Observatory has conducted 31
a number of investigations of the short wave radiation field. The basic principles underlying these investigations are the following:

1. It is necessary first to investigate the average optical state of the real atmosphere as a whole, or of typical isolated situations, and then to find the nature of the distribution of specific states about the average.

2. The theoretical description of the average state should be formulated with maximum utilization of physical data on the state of the atmosphere and the optical properties of its individual constituents; only when such data are lacking are empirical relations invoked to complete the scheme.

3. The simplest possible methods are used to determine the initial values of the numerical parameters required for calculation according to the theoretical plan.

4. The accuracy of the analytical tools used in the theory must not be significantly greater than the accuracy of the experimentally determined initial parameters, with allowance made, of course, for possible error accumulation.

In 1954 and 1955, K. S. Shifrin and I. N. Minin investigated the theory of nonhorizontal visibility (ref. 1). Again in 1959, K. S. Shifrin, and N. P. Pyatovskaya published tables of the oblique visible range and luminance of the daytime sky for a wide spread in values of the parameters characterizing the physical state of the atmosphere (ref. 2). In a paper published by K. S. Shifrin and O. A. Avaste in 1960 (ref. 3), the spectral range of applicability of the theory was extended to 4μ. The present article summarizes briefly the results of these studies.

THEORY OF SHORT WAVE FLUXES IN THE VISIBLE REGION OF THE SPECTRUM

The fundamental concept propounded in reference 1 consists in the formulation of a coherent optical description of the real cloudless atmosphere, such

that if certain characteristics of the atmosphere are known they can be used to calculate any of the other characteristics. These specific characteristics, which describe a given optical state of the atmosphere, are based on actual observations. The following empirical laws can be used to complete the total description:

1) aerosol structure of the clear atmosphere (ref. 13);

2) spectral transparency of the atmospheric aerosol (ref. 14);

3) the shape of the scattering diagram for the atmosphere (ref. 15).

It is possible as a result to construct a very simple model enabling one to calculate for specific optical states of the atmosphere the spectral fluxes penetrating the atmosphere in any given direction, the oblique visible range of any object, etc.

The initial parameters, that must be determined experimentally, are the horizontal visible range on the earth S_0 and the optical thickness of the atmosphere $\tau_0(\lambda)$.

It is shown in reference 1 that the total scattering coefficient can be calculated from the equation

$$\sigma(z, \lambda) = \frac{a_0(\lambda_0)}{\lambda^4} e^{-\alpha z} + \frac{b_0(\lambda_0)}{\quad} e^{-\beta z}, \tag{1}$$

where α and β are coefficients characterizing the decay of Rayleigh and aerosol scattering with altitude, respectively; $a_0(\lambda_0)$ and $b_0(\lambda_0)$ are the Rayleigh and aerosol scattering coefficients, respectively, on the earth's surface at a wavelength $\lambda_0 = 0.550\ \mu$.

The optical thickness of the total atmosphere and the horizontal range of visibility are defined by the formulas 32

$$\tau_0(\lambda_0) = \int_0^\infty \sigma(z, \lambda_0)\, dz = \frac{a_0(\lambda_0)}{\alpha} + \frac{b_0(\lambda_0)}{\beta}, \tag{2}$$

$$S_0 = \frac{3{,}91}{a_0(\lambda_0) + b_0(\lambda_0)}. \tag{3}$$

From these equations, one can readily determine the coefficients characterizing aerosol scattering:

$$\left.\begin{aligned} b_0 &= \frac{3{,}91}{S_\gamma} - a_0(\lambda_0) \\ \beta &= \frac{b_0(\lambda_0)}{\tau_0(\lambda_0) - \frac{a_\gamma(\lambda_0)}{\alpha}} \end{aligned}\right\} \qquad (4)$$

The coefficients pertinent to Rayleigh scattering, $a_0(\lambda_0)$ and α, are calculated theoretically.

It is interesting to note that the optical thicknesses calculated according to equation (1) are in good agreement with the average optical thicknesses (fig. 1) obtained by M. V. Savost'yanova (ref. 4).

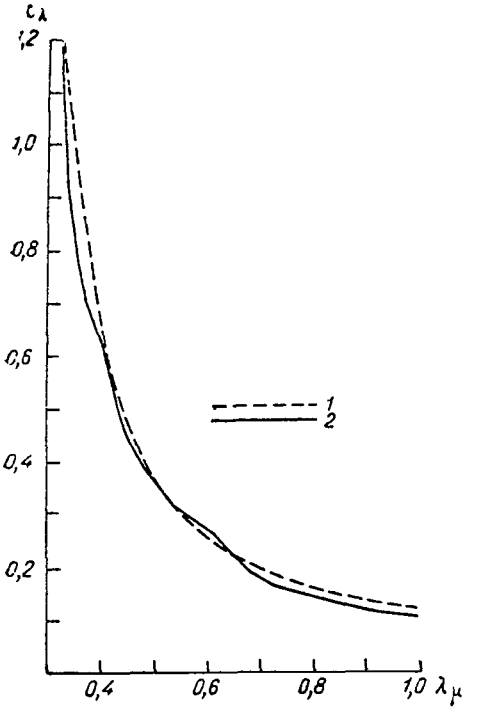

Figure 1. Wavelength Dependence of the Optical Thickness Under Average Conditions: 1) According to Equation (1) for $\tau_0 = 0.3$; 2) at Standard Atmospheric Transparency, According to Savost'yanova (ref. 4)

The most important factor in calculating the oblique visible range and luminance of the sky is the correct calculation of the luminance of the atmospheric haze, i.e., the intensity of light picked up by the instruments due to indirect scattering by the atmosphere. Calculation of the luminance of the atmospheric haze essentially involves solving completely the problem of radiation transport in the earth's atmosphere, taking into account the optical properties of the atmosphere itself as well as of the underlying surface.

In reference 1 an approximate method suggested by V. V. Sobolev in 1943 (ref. 5) is used to calculate the haze luminance. The equations for the haze luminance draw on the average polar scattering diagram of the real atmosphere. This diagram is determined by the relation

$$\varkappa(\gamma) = \frac{p}{\tau_0}\varkappa_R(\gamma) + \frac{q}{\tau_0}\varkappa_a(\gamma), \tag{5}$$

where

$$\frac{p}{\tau_0} + \frac{q}{\tau_0} = 1. \tag{6}$$

In this equation $\varkappa_R(\gamma)$ is the normalized Rayleigh index

$$\varkappa_p(\gamma) = \frac{3}{4}(1 + \cos^2\gamma); \tag{7}$$

γ is the scattering angle, $\varkappa_a(\gamma)$ is the aerosol scattering index (derived from the experimental data of reference 15).

For the relative optical thicknesses for Rayleigh and aerosol scattering, 33
we have

$$p = \frac{a_0(\lambda)}{\alpha}, \quad q = \frac{b_0(\lambda)}{\beta}. \tag{8}$$

The indices calculated from equation (5) are shown in figure 2 for two cases.

For many of the practical problems encountered in meteorology, engineering optics, biophysics, etc., one is required to know the luminance distribution over the entire sky. The experimental investigation of this problem is frought with considerable difficulties in connection with the tedious and time-consuming nature of the measurements. The approximate method of Sobolev provides sufficient accuracy in calculating the luminance of the sky.

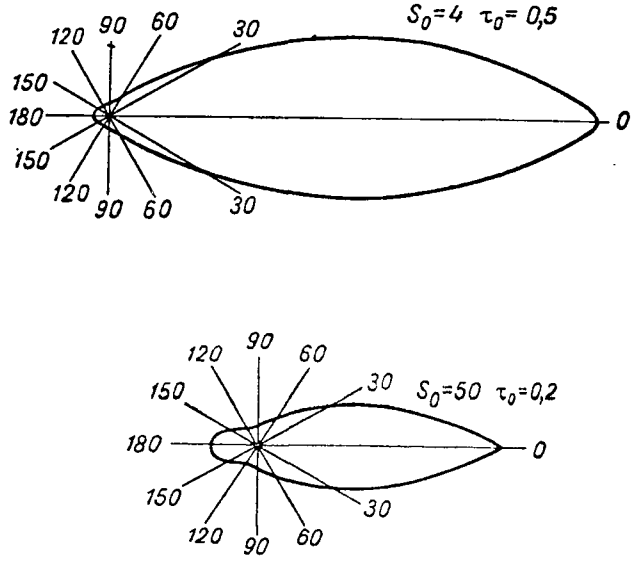

Figure 2. Average Scattering Indices of the Real Atmosphere

A comparison of the luminance values calculated in reference 2 for a clear sky with the experimental data of other authors (ref. 6-7) discloses satisfactory agreement in most cases. Figure 3 shows luminance isophots (in relative units) derived from theoretical data (curve 1) for the case when the horizontal visible range S_0 = 50 km, τ_0 = 0.2, the albedo A = 0.2, the zenith angle of the sun i = 60°; and according to the experimental data of Ye. V. Pyaskovskaya-Fesenkova (curve 2) (ref. 7). The theoretical and experimental isophots merge at the zenith, where the luminance of the sky is set equal to unity.

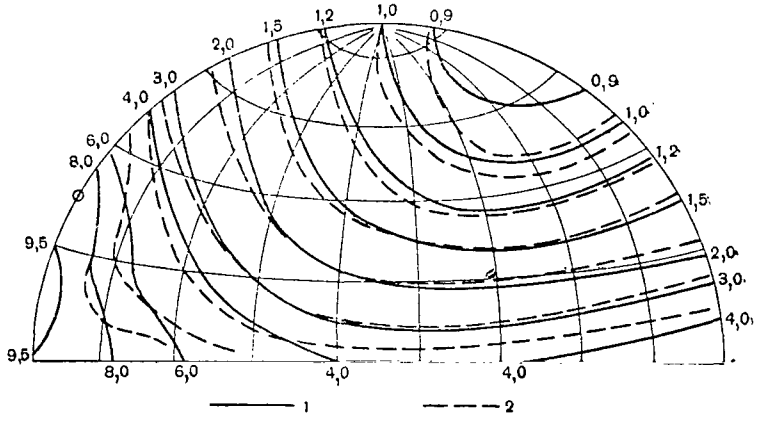

Figure 3. Luminance Isophots for a Clear Sky, Based on Theoretical (1) and Experimental (2) Data

It should be noted that the error in calculating the sky luminance by Sobolev's method is smaller when the transparency of the atmosphere is large (τ_0 small). This has also been confirmed by comparison of the theoretical calculations with the experimental results. Better agreement was obtained in those cases where the observations were made during high transparency of the atmosphere. A detailed error analysis of Sobolev's method is given in reference 8 by means of a comparison with numerical solutuions of the radiation transfer equation for an anisotropically scattering medium (ref. 9). The results obtained in reference 8 are summarized as follows:

1. When used for calculation of the downward intensities, Sobolev's method yields values that are too low at small scattering angles and too high at scattering angles approaching 90°, i.e., the extremums in the sky luminance distribution tend to smooth out. 34

2. The error of Sobolev's method in calculating the downward intensities is maximum at scattering angles near 90° (i.e., at the minimum of the sky luminance distribution). The error increases with increasing optical thickness of the atmosphere and with elongation of the scattering diagram.

3. For only slightly elongated scattering diagrams ($\kappa_1 = 1.0$ - ref. 8) the error of Sobolev's method applied to the calculation of the downward intensities is less than the simulation error of a synthetic atmosphere (single layer model, weighted scattering index), provided $\tau_0 < 0.5$.

The error in calculating the downward intensities is large only for a relatively narrow interval of scattering angles (in the vicinity of 90°). In the remaining angular interval, the error in Sobolev's method is substantially less. In both cases, Sobolev's method and the method of successive approximations used in the Internation Geophysical Year (IGY) calculations, the scattering index used for the analysis of single scattering is expanded in Legendre polynomials. Eleven terms are retained in the expansion.

It is important to realize that the error in this expansion is 10 to 15%, which induces the same error in the intensity at small optical thicknesses ($\tau_0 = 0.2$), because in calculating the single scattering case an inaccurate scattering index is used. At an optical thickness of $\tau_0 = 0.4$ the error of the method of successive approximations (in the IGY calculations) is 5%, but the error incurred in stopping with eleven terms of the expansion in Legendre polynomials amounts to ten percent.

4. The error of Sobolev's method in calculating the upward intensities is considerably less than for the downward intensities. For example, in the case of upward fluxes with a greatly elongated scattering diagram ($\kappa_1 = 2.0$) and a large optical thickness ($\tau_0 = 0.8$) the error is 15% smaller. It follows from the above that under average atmospheric conditions the error of Sobolev's method is comparable with the error generated in the method of successive

approximations when eleven terms are retained in the expansion of the scattering index.

Hence, in many practical applications, Sobolev's method provides satisfac- 35
tory accuracy under average atmospheric conditions.

It is possible, by Sobolev's method, to calculate very simply the albedo dependence of the atmospheric haze luminance. Some of the results are illustrated in figure 4 (borrowed from reference 6), which shows the dependence of the atmospheric haze luminance D on the albedo in the case when S_0 = 50 km, τ_0 = 0.2, i = 40°, ϕ = 90°, the sighting angle θ = 60°. It is seen in figure 4 that D(A) rises approximately linearly over the entire range of A, especially in the interval from A = 0 to 0.75. Consequently, where only rough estimates are needed, the function D(A) can for any values of A be replaced by a straight line. For more accurate calculations, it is necessary to resort to tables (ref. 1-2).

A very important problem, which can be solved by the method described in reference 1, is to calculate the nonhorizontal visible range.

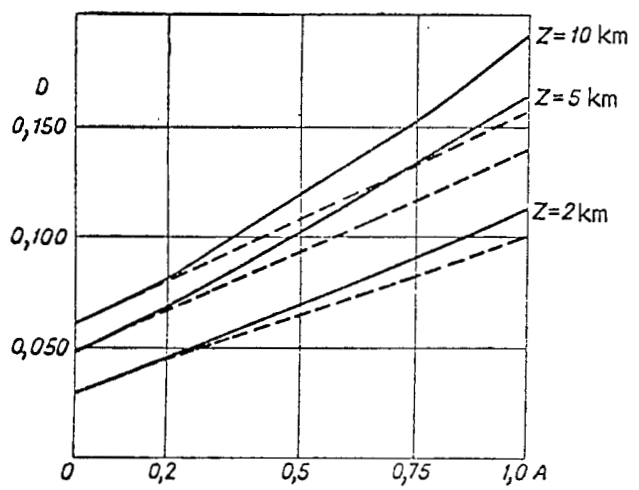

Figure 4. Luminance of the Atmospheric Haze as a Function of the Albedo; the Solid Curves Represent the True Function D(A), the dashed Curves Represent its Linear Approximation

The visibility of an object, of course, is dependent on whether the contrast K of the object against its background is greater than threshold contrast ϵ. The initial contrast between object and background diminishes on the path from object to observer due to haze in the atmosphere. The value of K depends, then, on the sighting angle or on the visible range L of the object. The range L is determined from the relation

$$K(L) = \varepsilon \tag{9}$$

or, in explicit form,

$$L = K^{-1}(\varepsilon). \tag{10}$$

A method is developed in reference 1 for evaluating the oblique visible range for visual observations on the basis of the spectral sensitivity curve of the eye. The given theory can be used equally well for any other receptor by introducing an appropriate sensitivity curve. An example is given in figure 5, which shows the contrast curves for sighting at various altitudes. At K = 2% (threshold value) we find values of the oblique visible range L = 8.5, 36 14.9, 57.5 km for altitudes of 1. 2, and 10 km, respectively.

In reference 10, Avaste estimates the error in calculating the oblique visible range. It is found that the error in the nonhorizontal visible range is governed mainly by the error in calculating the haze luminance. These errors are identical and under average atmospheric conditions amount to about ten or fifteen percent.

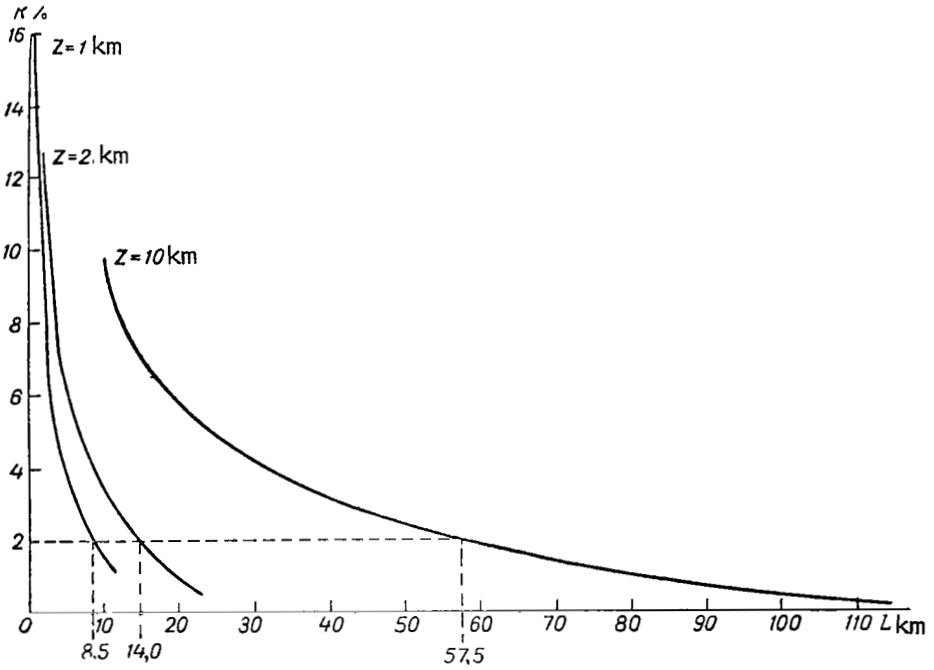

Figure 5. Variation in Contrast with Sighting from Various Altitudes

Yu. I. Rabinovich (ref. 1) has made a direct experimental check on the suitability of the theoretical scheme for describing average conditions in the real atmosphere. It turned out that in 85% of the cases the spectral contrasts predicted from the calculations were consistent with the measured values within an error of no more than 20%.

THEORY OF SHORT WAVE FLUXES IN THE INFRARED REGION OF THE SPECTRUM

The results presented above pertain to the visible region of the spectrum. A method is given by Shifrin and Avaste (ref. 3) for calculating the fluxes in the near infrared region. A plane-parallel model of the atmosphere beneath

the ozone layer is discussed. The average ozone content is assumed equal to 0.25 atm·cm (i.e., the thickness of an equivalent ozone layer in centimeters at standard pressure and temperature). The radiation is scattered by air molecules (Rayleigh atmosphere) and by the aerosol. It is assumed that the aerosol consists of two particles. The concentration of the large-particle aerosol decays exponentially with height, the concentration of fine aerosol remains constant in the troposphere. In the near infrared region absorption by water vapor and carbon dioxide gas is taken into account. Accounting simultaneously for both the absorption of short wave radiation by water vapor and carbon dioxide as well as scattering imposes enormous difficulties in that, first, the absorption bands have a complex structure (they consist of partially overlapping absorption lines whose width is pressure dependent) and, second, the water vapor and gaseous carbon dioxide concentration varies with height according to laws that differ from the law governing the concentration of scattering particles as a function of height. 37

The water vapor concentration decreases exponentially with height. The overall content of water vapor in a vertical column varies from 0.5 to 3.0 cm at medium latitudes; the mean value is 2.1 cm.

The volume concentration of carbon dioxide gas is constant (0.03%). To account for the effect of pressure on absorption, a model of the atmosphere is used in which the virtual temperature falls off linearly with height, i.e., the model is almost identical to a polytropic atmosphere. Due to the Forbes effect, the absorption coefficients for water vapor and carbon dioxide can only be applied to strictly monochromatic radiation. The absorption coefficients found in the literature for water vapor and carbon dioxide gas are not comparable, since the experimental conditions (quantity of gas absorbed on the ray path, absorption bandwidth, pressure, temperature) have been different. It is more suitable to make use of emprically determined absorption functions.

The results of a scrupulous study of absorption in the near infrared region of the spectrum in a so-called synthetic atmosphere were published in 1956 by Howard, Burch, and Williams (HBW) (ref. 16-20).

An analysis of the HBW experimental data shows that the average abosrption function for the water vapor and carbon dioxide bands may be represented correct to 5% by the formulas:

$$A(x) = \frac{1}{\nu_2 - \nu_1} \int_{\nu_1}^{\nu_2} A_\nu \, d\nu, \tag{11}$$

$$A(x) = cx, \quad \text{если} \quad x < x_{cr}$$

$$A(x) = C + D \lg x, \quad \text{если} \quad x > x_{cr} \tag{12}$$

where the parameter

$$x = \sqrt{w}\,(P + e)^n. \tag{13}$$

Here ν_1, ν_2 are the edge frequencies of the band, w is the content of absorbed gas on the ray path, P is the total pressure, e is the partial pressure

of the absorbed gas, c, C, D, x_{cr} are constants typical of the given absorption band and are derived from the experimental data, n is a constant depending on the width of the spectral interval.

Under the conditions anent the HBW experiment $n \approx 0.3$ for water vapor, $n \approx 0.4$ for carbon dioxide. The results of a calculation of the absorption function A(x) for water vapor are shown in figure 6. The absorption functions A(x) for the Ω, Ψ, X, and 3.2μ bands were calculated according to equations (12, (13) using the HBW values (ref. 16-20). The absorption functions for the 0.7 and 0.8μ, $\rho\sigma\tau$, and Φ bands were obtained from the data of Fowler; because in all of the HBW measurements of the $\rho\sigma\tau$ and Φ bands the water vapor content along the ray path was small (ref. 3).

The discrepancies between the HBW and Fowler absorption functions for the $\rho\sigma\tau$ and Φ bands are clearly attributable to the fact that Fowler assumed the edges of these absorption bands to be wider apart than in the work of Howard, Burch, and Williams.

Correct to 10%, the absorption function can be represented by the single formula

$$A(x) = \frac{x}{ax + b}, \tag{14}$$

where α and β are constants.

The results of calculations based on equation (14) are plotted point by point in figure 6. Analogous curves were generated for carbon dioxide. 38

The transmission function was calculated from the relation T = 1 - A(x).

In order to render the HBW constant pressure data applicable to actual atmospheric conditions, we introduce the weighted average pressure, which is obtained from the equation

$$\overline{(P+e)^n}\Big|_{z_1}^{z_2} = \frac{\int_{z_1}^{z_2} \eta(z)\,(P+e)^n\,dz}{\int_{z_1}^{z_2} \eta(z)\,dz}, \tag{15}$$

where $\eta(z)$ is the density of the absorbing gas.

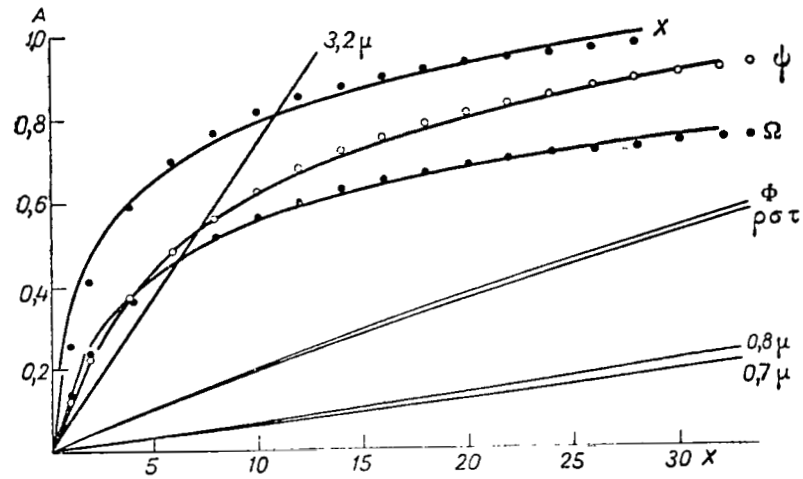

Figure 6. Absorption in the Water Vapor Bands as a Function of the Parameter x

For the atmosphere in question, the weighted average pressure is obtained for water vapor and carbon dioxide from the respective equations

$$P_{\text{wt H}_2\text{O}} \approx \frac{7}{9} P(z), \tag{16}$$

$$P_{\text{wt CO}_2} \approx \frac{3}{7} P(z), \tag{17}$$

where P(z) is the pressure at height z.

The authors calculated the intensity of direct solar radiation at various levels. The calculations were made for three quantities of precipitated water w (0.5, 2.1, and 3 cm) at different elevations of the sun, utilizing the data of Johnson (ref. 2) for the spectral intensities of extra-atmospheric solar radiation.

The following equation was used to calculate the direct radiation:

$$S(z, m) = \int_0^\infty I_0(\lambda)\, e^{-m\left[\tau_z^\infty(\lambda) + k_{\lambda, O_3} w\right]} T\left(\bar{x}_w \sqrt{m}\right) T\left(\bar{x}_{CO_2} \sqrt{m}\right) d\lambda - \tag{18}$$

$$- f_3(m) \frac{S_m(z)}{S_{m,\mathrm{id}}(z)},$$

where $I_0(\lambda)$ is the solar radiation flux density incident on the upper boundary of the atmosphere, m is the mass of the atmosphere, k_{λ, O_3} is the monochromatic

absorption coefficient for ozone, $T(\overline{x}_w)$ is the average transmission function in 39
the water vapor absorption band, $T(\overline{x}_{CO_2})$ is the average transmission function in the carbon dioxide absorption band, $S_m(z)$ is the integral flux of direct solar radiation in the real atmosphere at the atmospheric mass $\underline{m}$, $S_{m,id}(z)$ is the same for an ideal atmosphere, $f_3(m)$ is a correction for absorption by permanent gases.

In the ultraviolet and visible regions of the spectrum, the method outlined in reference 1 is used to calculate the fluxes. In the infrared region of the spectrum, the absorption and scattering are simultaneously accounted for to a first approximation by considering only single scattering and approximating the real atmosphere by a stratified model comprising eight layers. We postulate that scattering events take place only in the centers of mass of the layers. The calculated spectral flux of scattered radiation is shown in figure 7 as a function of wavelength. It is apparent in the figure that the intensity of scattered radiation is negligibly small at the earth's surface for $\lambda > 2\mu$.

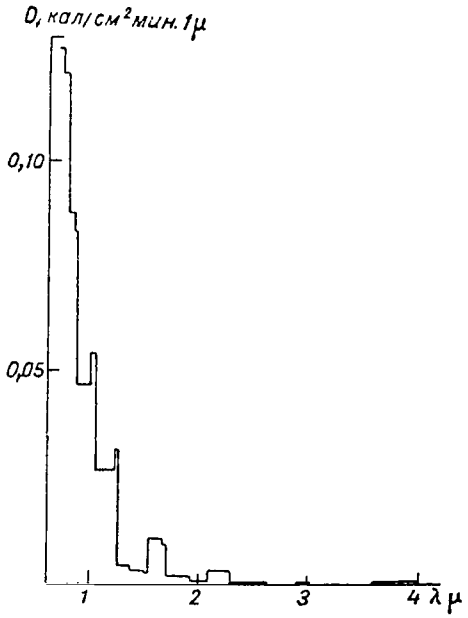

Figure 7. Spectral Flux of Scattered Radiation as a Function of Wavelength for z = 0 km, Atmospheric Mass m = 2, Albedo A = 0, $\tau_0 = 0.3$, w = 2.1 cm

Assuming a radiation scattering of 100% in the interval $0.7\mu < \lambda < 4\mu$, the scattered radiation in the interval $\lambda > 2\mu$ is less than 1% of the total. With the proposed model of the atmosphere, the scattered radiation intensity, beginning at 2 km, falls off almost linearly with height to the tropopause. Above

11 km essentially the only scattering left is caused by air molecules, and the scattered radiation flux begins to decline exponentially. Under the presumed average atmospheric conditions, we find at the earth's surface, taking absorption into account, that the decrease in scattered radiation is about 5% of the absorbed direct solar energy. This means that in calculating the radiation heating of the air, it is justifiable in the first approximation to neglect the absorption of scattered radiation by water vapor, since the influence of the latter amounts to just a few percent of the direct solar energy absorbed by water vapor, and the relative contribution of scattered radiation to the total flux diminishes with height.

It is to be noted that the curves shown in figure 7, for the distribution of spectral flux with respect to wavelength, were obtained with the albedo equal to zero. The approximate growth of the scattered radiation flux in the near infrared due to increasing reflection from the earth's surface is obtained from the equation

$$\Delta F_D = \int_{0,7\mu}^{\infty} (F^0_{D,\lambda} + S'_\lambda) \frac{\tilde{\lambda} A_\lambda}{\frac{4}{a\tau_{0,\lambda}} + 1 - A_\lambda} d\lambda, \tag{19}$$

where

$$\tilde{\lambda} = \frac{\tau_{0,\lambda} \overline{\sec\theta}}{\tau_{0,\lambda} \overline{\sec\theta} - \ln\left[T\left(x \sqrt{\overline{\sec\theta}}\right)\right]}, \tag{20}$$

40

$$a = 3 - \tilde{\lambda} \varkappa_1, \qquad \varkappa_1 = \frac{3}{2} \int_0^{\pi} \varkappa(\gamma) \sin\gamma \cos\gamma \, d\gamma,$$

$$T\left(x \sqrt{\overline{\sec\theta}}\right) = 1 - A\left(x \sqrt{\overline{\sec\theta}}\right), \tag{21}$$

$\tau_{0,\lambda}$ is the spectral optical thickness of the scattering atmosphere (air molecules, aerosol), $\overline{\sec\theta}$ = 1.66 is the mean secant (diffusivity), S'_λ is the spectral flux of direct solar radiation on the horizontal surface, $F^0_{D,\lambda}$ is the spectral flux of scattered radiation with the albedo A = 0. Figure 8 shows the dependence of the total scattered radiation flux on the solar zenith angle.

Making use of Dirmhirn's data for A_λ (23) in combination with equation (19), we find that there is very little difference (less than 0.5%) in the infrared scattered radiation fluxes between summer and winter under average conditions. Also shown in figure 8 are the results of observations of the total flux (visible + infrared) of scattered radiation in the city of Tartu (Estonia)

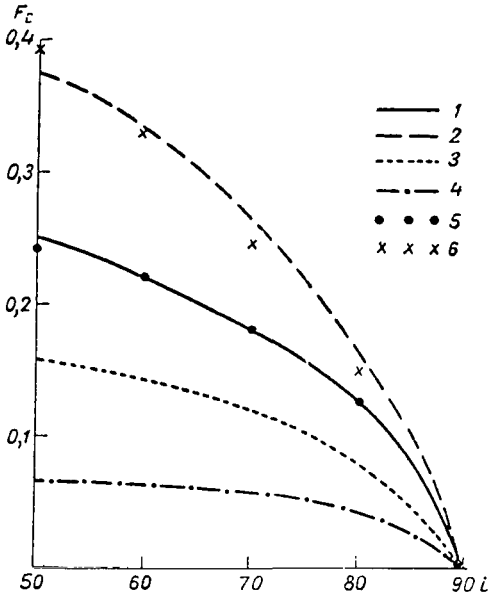

Figure 8. Total Scattered Radiation Flux as a Function of Solar Zenith Angle:

1) Tartu in summer with trubidity factor T = 3;
2) Tartu in winter with turbidity factor T = 3;
3) In the visible region of the spectrum $\lambda<0.7\mu$ with $\tau_0 = 0.3$, A = 0;
4) Average scattered radiation flux (summer and winter) in the infrared region $\lambda>0.7\mu$ with $\tau_0 = 0.3$, w = 2.1 cm;
5) Calculated total scattered radiation flux in the visible region with $\overline{A_S} = 0.1$, $\tau_0 = 0.3$, w = 2.1 cm;
6) Calculated total scattered radiation flux in the visible region with $\overline{A_W} = 0.8$, $\tau_0 = 0.3$, w = 2.1 cm.

during summer and winter with an average turbidity factor T = 3 (curves 1 and 2). Assuming that in the visible region the winter albedo $\overline{A}_W = 0.8$, and the summer value $\overline{A}_S = 0.1$, curves 5 and 6 are obtained. Curve 3 shows the behavior of the total flux in the visible region of the spectrum for A = 0. All of the values in figure 8 are given in relative units. The fluxes can be converted to cal/cm^{2}min by multiplying the dimensionless quantities by $\frac{I}{\kappa}$°. It is impossible to compare the results shown in figure 8 with the experimental data, because the calculations were made for a water vapor content w = 2.1 cm. This value is a fairly realistic measure of the average conditions in summer, but in winter the value of w is far less. The good agreement between the calculated and measured fluxes implies that the relative increase in total scattered radiation flux in winter over summer, given the same elevation of the sun and atmospheric tur-

bidity, is attributable to the large values of the albedo in winter specifically 41
in the visible portion of the spectrum.

Finally, the authors performed a calculation of the scattered radiation isophots in the near infrared region of the spectrum in the absorption bands and outside of them, assuming that only scattering occurs. The water vapor content was w = 2.1 cm. The calculations were made using the standard radiation model of the atmosphere (fig. 9-14). In each of the figures, the fraction seen near the top of the graph gives the maximum value of the scattered radiation intensity outside the absorption band (numerator) over the same value in the absorption band (denominator).

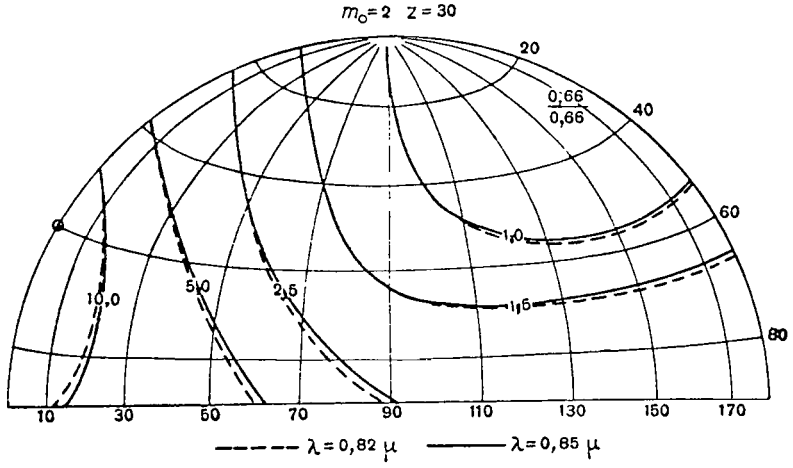

Figure 9. Scattered Radiation Isophots in the Absorption Band $\lambda = 0.82_\mu$ and Outside the Band $\lambda = 0.85_\mu$ for m = 2, z = 3 km

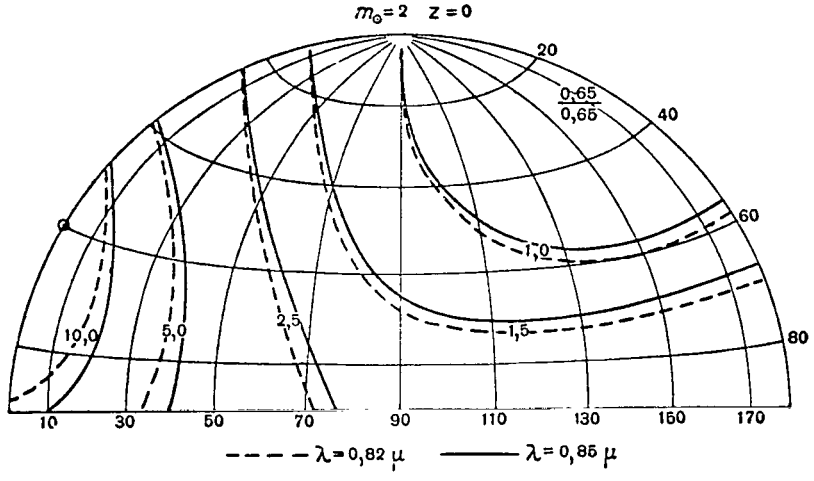

Figure 10. Scattered Radiation Isophots in the Absorption Band $\lambda = 0.82_\mu$ and Outside the Band $\lambda = 0.85\ \mu$ for m = 2, z = 0 km

It is evident in the figures that as the surface of the earth is approached, the absorption increases. Thus, for a weak band ($\lambda = 0.82\ \mu$) the absorption is insignificant at a height of 3 km (fig. 9), but on the earth's surface the drop in intensity due to absorption at large zenith angles comes to 10% (fig. 10-11). In the strong Ψ band ($\lambda = 1.31\ \mu$) the reduction in scattered radiation intensity due to absorption at large zenith angles is about 20% at a height of 3 km (fig. 12), about 50% at the surface of the earth (fig. 13-14); for a more detailed discussion, see reference 12.

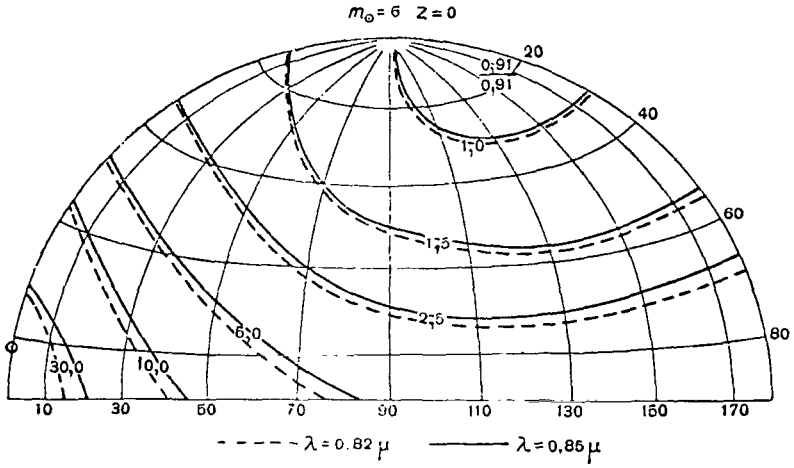

Figure 11. Scattered Radiation Isophots in the Absorption Band $\lambda = 0.82\mu$ and Outside the Band $\lambda = 0.85\mu$ for m = 6, z = 0 km

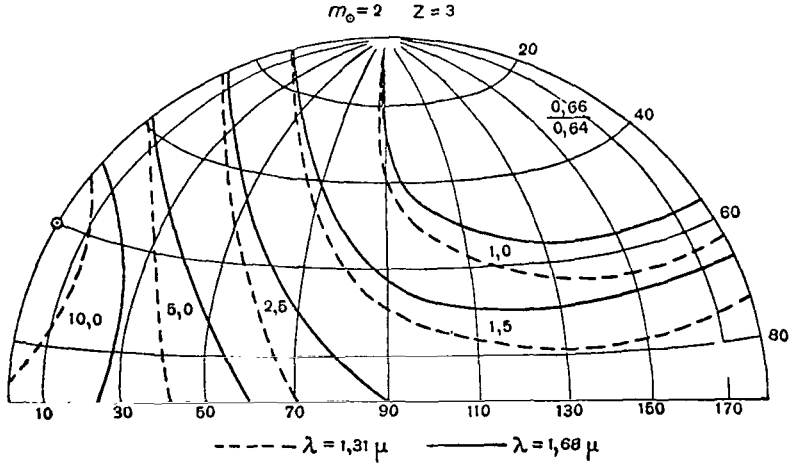

Figure 12. Scattered Radiation Isophots in the Absorption Band Ψ ($\lambda = 1.31\ \mu$) and Outside the Band $\lambda = 1.68\mu$ for m = 2, z = 3 km

A comparative analysis of the calculated isophots and the experimental data published by Oetjen, et al. (ref. 21-22) exhibits satisfactory agreement between the intensity values at the zenith. Oetjen, however, obtained a deeper minimum in the sky luminance distribution at a scattering angle of 90°. This means that in the near infrared region, the scattering curve is more elongated than in the visible region (for the calculations the authors used weighted average scattering indices derived from measurements in the visible portion of the spectrum).

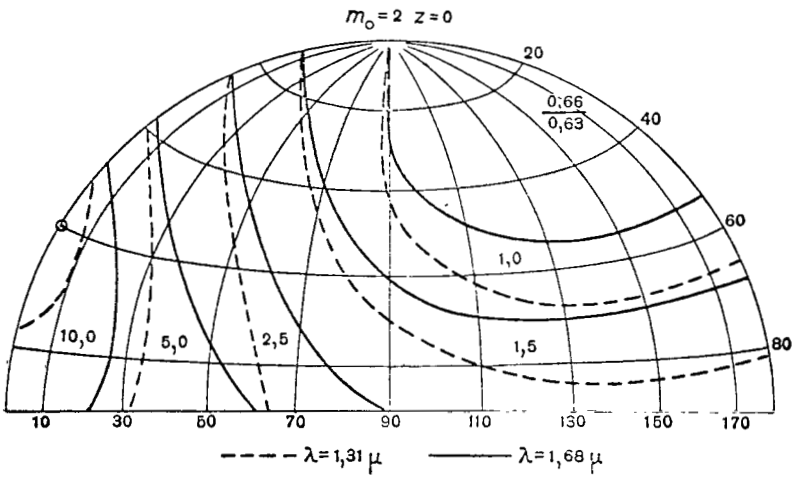

Figure 13. Scattered Radiation Isophots in the Absorption Band Ψ (λ = 1.31 μ) and Outside the Band λ = 1.68 μ for m = 2, z = 0 km

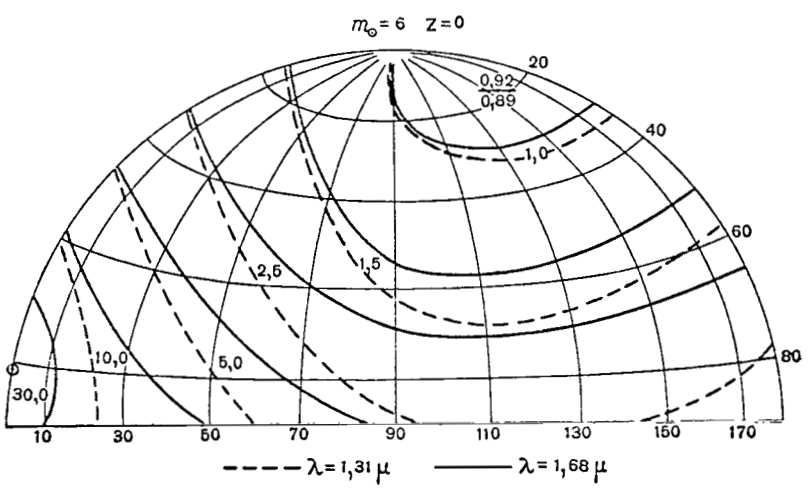

Figure 14. Scattered Radiation Isophots in the Absorption Band Ψ (λ = 1.31 μ) and Outside the Band λ = 1.68 μ for m = 6, z = 0 km

We note that elongation of the atmospheric scattering curve with increasing wavelength is a direct consequence of the theoretical scheme outlined in reference 1. As λ increases, the aerosol contribution q/τ_0 increases appreably over the Rayleigh contribution p/τ_0, so that, in accordance with equation (5), the average atmospheric scattering curve becomes greatly elongated. Hence, for S_0 = 20 km and τ_0 = 0.3 we obtain table 1, which illustrates the degree of elongation of the scattering curve. This effect is discussed in further detail in reference 12. 43

TABLE 1

λ_μ	$\frac{p}{\tau_0}$	$\frac{q}{\tau_0}$	$\frac{\varkappa(0)}{\varkappa(90)}$	$\frac{\varkappa(180)}{\varkappa(90)}$
0,400	0,554	0,446	11,6	1,69
0,550	0,317	0,683	20,1	1,50
0,800	0,129	0,871	27,8	1,17

Conclusion 44

Our investigations have led to the formulation of an optical model of the real cloudless atmosphere, wherein maximum use is made of those parameters which are most readily amenable to measurement (τ_0, S_0, w).

A simple method has been proposed for calculating the intensities and fluxes with satisfactory accuracy insofar as a large number of important practical problems are concerned.

REFERENCES

1. Shifrin, K.S. and Minin, I.N. Theory of Nonhorizontal Visibility (K teorii negorizontal'noy vidimosti). Trudy Glavnoy Geofizicheskoy Observatorii (GGO), No. 68, 1957.

2. Shifrin, K.S. and Pyatovskaya, N.P. Tables of the Oblique Range of Visibility and Luminance of the Daytime Sky (Tablitsy naklonnoy dal' nosti vidimosti i yarkosti dnevnogo neba). Gidrometeoizdat, Leningrad, 1959.

3. Shifrin, K.S. and Avaste, O.A. Short Wave Radiation Fluxes in the Cloudless Atmosphere (Potoki korotkovolnovoy radiatsii v bezoblachnoy atmosfere). Research in Physics of the Atmosphere (Issledovaniya po fizike atmosfery), No. 2. Inst. Fiziki i Astronomii AN ESSR (Institute of Physics and Astronomy, Academy of Sciences of the Estonian SSR), 1960.

4. Savost'yanova, M.V. Spectral Composition of the Daytime Sky for Photography (Spektral'nyy sostav dnevnogo neba pri fotos"emke). Izv. Akad. Nauk SSSR, Ser. Geogr. i Geofiz., No. 4, 1942.

5. Sobolev, V.V. Approximate Solution to the Problem of Light Scattering in a Medium with an Arbitrary Scattering Diagram (Priblizhennoye resheniye zadachi o rasseyanii sveta v srede s proizvol'noy indikatrisoy rasseyaniya). Astron. Zhur., Vol. 20, Nos. 5-6, 1943.

6. Shifrin, K.S. and Pyatovskaya, N.P. Calculations of the Oblique Range of Visibility and Luminance of a Clear Sky (Raschety naklonnoy dal'nosti vidimosti i yarkosti bezoblachnogo neba). Trudy 2-go Mezhvedomstvennogo Soveshchaniya Aktinometrii i Atmosfernoy Optike. Gidrometeozdat, Leningrad, 1961.

7. Pyaskovskaya-Fesenkova, Ye. V. Investigation of Light Scattering in the Earths Atmosphere (Issledovaniye rasseyaniya sveta v zemnoy atmosfere). Izd. AN SSSR, Moscow, 1957.

8. Avaste, O.A. Approximation Error in Calculating the Luminance of Atmospheric Haze (O tochnosti priblizhennogo metoda rascheta yarkosti atmosfernoy dymki). Trudy 2-go Mezhvedomstvennogo Soveshchaniya po Aktinometrii i Atmosfernoy Optike. Gidrometeoizdat, Leningrad, 1961.

9. Feigel'son, Ye.M. Malkevich, M.S. Kogan, S. Ya., Koronatova, T.D., Glazova, K.S. and Kuznetsova, M.A. Calculation of Sky Luminance in an Atmosphere with Anistropic Scattering (Raschet yarkosti neba v atmosfere pri anizotropnom rasseyanii). Trudy Instituta Fiziki Atmosfery Akademii Nauk SSSR (IFA AN SSSR), Part 1, No. 1, 1958.

REFERENCES (continued)

10. Avaste, O.A. Approximation Error in Calculating the Oblique Range of Visibility (O tochnosti priblizhennoy skhemy rascheta naklonnoy dal'nosti vidimosti). Trudy GGO, No. 109, 1961.

11. Rabinovich, Yu. I. Experimental Verification of the Nonhorizontal Visibility Theory of K.S. Shifrin and I.N. Minin (Eksperimental'naya proverka teorii negorizontal'noy vidimosti K.S. Shifrina i I.N. Minina). Trudy Vsesoyuznogo Nauchnogo Meteorologicheskogo Soveshchaniya, Vol. 6, 1963.

12. Avaste, O.A., Moldau, Kh. and Shifrin, K.S. Spectral Distribution of Direct and Scattered Radiation (Spektral'noye raspredeleniye pryamoy i rasseyannoy radiatsii). Issledovaniya po Fizike Atmosfery, No. 3. Inst. Fiziki i Astronomii AN ESSR, 1962.

13. Penndorf, R. The Vertical Distribution of Mie Particles in the Troposphere. J. Meteorol., Vol. 11, No. 3, 1954.

14. Schmolinsky, F. Wavelength Dependence of the Visible Range and Vapor Extinction Coefficient (Die Wellenlängenabhängigkeit der Sichtweite und des Koeffizienten der Dunstextinktion). Meteorol. Z., Vol. 61, No. 6, 1944.

15. Foitzik, L. and Zschaeck, H. Measurement of the Spectral Scattering Function of the Ground Level Atmosphere Under Conditions of Good Visibility, Haze, and Overcast (Messungen der spektralen Zerstreuungsfunktion bodennaher Luft bei guter Sicht, Dunst und Nebel). Z. Meteorol., Vol. 7, No. 1, 1953.

16. Howard, J.H., Burch, D.E. and Williams, D. Infrared Transmission of Synthetic Atmospheres. I. Instrumentation. J. Opt. Soc. Am., Vol. 46, No. 3, 1956.

17. Howard, J.N., Burch, D.E. and Williams, D. Infrared Transmission of Synthetic Atmospheres. II. Absorption of Carbon Dioxide. J. Opt. Soc. Am., Vol. 46, No. 4, 1956.

18. Howard, J.N., Burch, D.E. and Williams, D. Infrared Transmission of Synthetic Atmospheres. III. Absorption by Water Vapor. J. Opt. Soc. Am., Vol. 46, No. 4, 1956.

19. Howard, J.N., Burch, D.E. and Williams, D. Infrared Transmission of Synthetic Atmospheres. IV. Application of Theoretical Band Models. J. Opt. Soc. Am., Vol. 46, No. 5, 1956.

20. Howard, J.N., Burch, D.E. and Williams, D. Infrared Transmission of Synthetic Atmospheres. V. Absorption Laws for Overlapping Bands, Vol. 46, No. 6, 1956.

21. Oetjen, R.A., Bell, E.E., Young, J. and Eisner, L. -Spectral Radiance of Sky and Terrain at Wavelengths Between 1 and 20 Microns. I. Instrumentation. J. Opt. Soc. Am., Vol. 50, No. 12, 1960.

22. Bell, E.E., Eisner, L., Young, J. and Oetjen, R. Spectral Radiance of Sky and Terrain at Wavelengths Between 1 and 20 Microns. II. Sky Measurements. J. Opt. Soc. Am., Vol. 50, 12, 1960.

23. Dirmhirn, I. Spectral Distribution of the Reflection from Natural Media (Zur spektralen Verteilung der Reflexion natürlichen Medien). Wetter und der Leben, Vol. 9, No. 3-5, 1957.

STEMAR ENGINEERING, INC.
(James S. Wood, Translator)

NASA-Langley, 1965 F-272

"The aeronautical and space activities of the United States shall be conducted so as to contribute . . . to the expansion of human knowledge of phenomena in the atmosphere and space. The Administration shall provide for the widest practicable and appropriate dissemination of information concerning its activities and the results thereof."

—NATIONAL AERONAUTICS AND SPACE ACT OF 1958

NASA SCIENTIFIC AND TECHNICAL PUBLICATIONS

TECHNICAL REPORTS: Scientific and technical information considered important, complete, and a lasting contribution to existing knowledge.

TECHNICAL NOTES: Information less broad in scope but nevertheless of importance as a contribution to existing knowledge.

TECHNICAL MEMORANDUMS: Information receiving limited distribution because of preliminary data, security classification, or other reasons.

CONTRACTOR REPORTS: Technical information generated in connection with a NASA contract or grant and released under NASA auspices.

TECHNICAL TRANSLATIONS: Information published in a foreign language considered to merit NASA distribution in English.

TECHNICAL REPRINTS: Information derived from NASA activities and initially published in the form of journal articles.

SPECIAL PUBLICATIONS: Information derived from or of value to NASA activities but not necessarily reporting the results of individual NASA-programmed scientific efforts. Publications include conference proceedings, monographs, data compilations, handbooks, sourcebooks, and special bibliographies.

Details on the availability of these publications may be obtained from:

SCIENTIFIC AND TECHNICAL INFORMATION DIVISION

NATIONAL AERONAUTICS AND SPACE ADMINISTRATION

Washington, D.C. 20546